MODELING BRISTLE LIFT-OFF IN IDEALIZED BRUSH SEAL CONFIGURATIONS

VIJAY MODI
DEPARTMENT OF MECHANICAL ENGINEERING
COLUMBIA UNIVERSITY
NEW YORK, NEW YORK 10027

1. Introduction

In the last decade, brush seals have emerged to be one of the most promising technologies for the reduction of leakage flow in gas turbine engines. Recent bench tests indicate a possibility of an order of magnitude reduction in leakage flow over multiknife labyrinth seal, Holle and Krishnan (1990). Additional potential for performance benefit arises from mechanical and maintenance considerations. The efficiency of a labyrinth type seal depends upon the clearance between the tip of the knife and the bore but this radial clearance may be difficult to control due to thermal and dynamic conditions. A brush seal on the other hand is compliant, and hence has the ability to recover after excursions, Flower (1990). An important question that remains to be answered is the relationship between brush configuration/operation parameters and some measure of its compliance. One measure of compliance is the clearance that develops between the bristle tips and the rotating element due to the pressure differential across the seal and due to the aerodynamic drag.

We attempt in this paper to develop a model for the flow through brush seals and determine their elastic behavior in order to predict the dependence of brush/journal clearance on geometry and operating conditions. Several idealizations regarding brush seal configuration, flow conditions and elastic behavior are made in the analysis in order to determine closed form parametric dependence. This formulation assumes that there is no initial interference between the bristle tip and the rotor. Also interbristle, bristle-backing plate and bristle-rotor friction is neglected. The bristle bundle or the brush seal as it is alternately called is assumed homogeneous and isotropic on a macroscopic scale so that a physical property like permeability is uniform. The fluid is assumed to be homogeneous, incompressible, viscous and is flowing under steady conditions.

A schematic of a brush seal is shown in figure 1. If the nominal bristle-shaft interference is absent then under static conditions the bristles may deflect axially due to the imposed pressure differential. This axial deflection may create a clearance permitting leakage flow in excess of that which occurs through the porous matrix

formed by the bristle bundles. Under dynamic conditions the Couette flow created by shaft motion could be strong enough to cause bristle deflection and once again a clearance may develop.

The paper proposes a means to determine this clearance (or at least describe its parametric dependence on geometry and operating conditions) under static as well as dynamic conditions. The study can be thought of as consisting of three separate modeling efforts. First a flow model that describes the coupled parallel flow through the porous medium made of bristle bundles and the clearance region. This development follows the earlier work of Beavers and Joseph (1967), Beavers et al. (1970), Williams (1978) and Rudraiah (1985). This model provides the macroscopic description of the flow field, i.e., a filter velocity in the porous medium. Second, a model to relate this macroscopic flow field to a local flow field and its associated drag on the bristle is developed. This model also permits us to determine an expression for the permeability in order to characterize the physical property of the bristle bundle in absence of an experimentally determined value. The forces on a single bristle due to this macroscopic flow field are then estimated assuming idealized microscopic flow behavior and a phenomenological description of drag on a bristle. Third, the elastic behavior is modeled to estimate the deflection of the bristle tip due to the flow field or the impressed axial pressure differential. A description of the clearance would in principle require a simultaneous solution of the three models. It is, however, assumed here that the physical property permeability remains unchanged both due to the presence of leakage flow through and around the bristle bundle as well as due to the deformation of the bristles themselves. Given this, it is then necessary to solve only the flow and elastic models simultaneously to determine the clearance.

2. Circumferential Deflection

To determine the circumferential deflection of the bristles we must first estimate the forces on each bristle. The forces in the circumferential direction are due to drag caused by the flow around the bristle bundle. This flow is in turn driven by the Couette flow in the bristle-shaft clearance as a result of the circumferential slip velocity of the shaft itself. In the absence of a clearance, the shaft motion imposes a circumferential velocity boundary condition directly at the bristle-shaft interface. A model to determine the flow field in both these circumstances is introduced next. This development assumes that the clearance h_0 if any is known. Its actual value will be determined later along with considerations of the elastic behavior.

2.1 Flow Model

Let us consider the geometry shown in figure 2, with a porous medium of height h underlying a channel formed by a clearance of height h_0. The clearance is bounded above by an impermeable wall moving to the right at u_0 and the porous region is bounded below by an impermeable stationary wall. The formulation presented here follows that in Rudraiah (1985). The basic equations describing the flow are obtained after the following approximations are made.

i)   The fluid is homogeneous and incompressible.

ii) The flow in the channel and in the porous medium is driven by a shear produced due to the motion of the upper plate. This flow is steady, laminar and fully developed.

iii) The porous medium formed of bristle bundles is homogeneous and isotropic on a macroscopic scale.

iv) The flow in the porous medium is adequately described by the Brinkman equations and this flow is coupled to the channel flow by a boundary condition given by Williams (1978).

Following Rudraiah (1985), we write equations for u, velocity in the gap and $\hat{u}$, filter velocity in the porous medium as:

$$\frac{d^2u}{dy^2} = 0 \quad \text{and} \quad \frac{d^2\hat{u}}{dy^2} - \frac{1}{\lambda k} \, u = 0 \tag{1}$$

where λ is a positive constant and k is the permeability of the porous medium. The velocity $\hat{u}$ in the porous medium is related to u by

$$u = (1-\phi) \, \hat{u} \tag{2}$$

where $(1-\phi)$ is the porosity. Following Williams (1978), at the clearance-porous medium interface we assume that:

$$\frac{du}{dy} = (1-\phi)\lambda \, \frac{d\hat{u}}{dy} \tag{3}$$

The remaining boundary conditions are the usual no-slip conditions at impermeable walls and are:

$$u = u_0 \quad \text{at} \quad y = h_0$$
$$u = 0 \quad \text{at } y = -h \tag{4}$$

Solving (1) subject to (2), (3) and (4) we obtain the velocity distributions in the clearance and the porous regions to be

$$u = u_0 \left[1 - \frac{\lambda\delta\,(h_0 - y)}{(\tanh\delta h + \lambda\delta h_0)} \right] \quad y > 0$$

$$\hat{u} = \frac{u_0}{(1-\phi)(\tanh\delta h + \lambda\delta h_0)} \left[\sinh\delta y + \frac{\cosh\delta y}{\coth\delta h} \right] \quad y < 0 \tag{5}$$

where $\delta = (\lambda k)^{-1/2}$. Here $\delta h = h\,(\lambda k)^{-1/2} \gg 1$ is used. This relies on λ to be of order unity and h to be a macroscopic length scale assumed to be several times greater than $k^{1/2}$ (which is typically of order d_0, the characteristic dimension of the porous matrix, i.e. bristle diameter). Hence we may approximate $\hat{u}$ by

$$\hat{u} = \frac{u_0}{\eta}\, e^{\delta y} \quad\quad y < 0 \tag{6}$$

where $\eta = (1-\phi)(1+\lambda\delta\,h_0)$. The exponential behavior of the filter velocity implies that it decays to the Darcy value (which in this case is zero) within a boundary layer of length scale $1/\delta$, where $1/\delta$ is of the order of $k^{1/2}$.

Here $\hat{u}$ represents a filter velocity, a macroscopic quantity defined in order to avoid the more difficult question of what is the true velocity of the fluid in the porous region between the bristles. We now make certain idealizations about the bristle bundle geometry and subsequently model the flow through the interbristle pores in order to determine the viscous drag force directly as a function of the filter velocity.

2.2.   Permeability Model

The drag force on a bundle of cylindrical bristles clearly depends upon the flow through the pores which in turn depends upon the particular geometric configuration. Let us first examine the situation for two particular geometric arrangements. Let us assume that the cross-section of the bundle remains same in the direction along the bristle axis and that the flow is normal to these axes. Let ϕ be the solidity or here the area fraction and Z be the number of nearest neighbors.

Then ϕ and Z are respectively $\pi/4 = 0.79$ and 4, for a square array and $\pi/2\sqrt{3} = 0.907$ and 6 for a hexagonal array. For these arrays there is no possibility of any transverse flow since all neighboring cylinders are in contact. Typical solidities ϕ for brush seals are between 0.7 and 0.8, indicating a fairly close packed geometry. It is very likely that the manufacture of bristle bundles and their relative movement in the presence of leakage flow lead to bristle configurations that are close to random. A particular means to generate a closely packed random array is by the following two step process, described by Sangani and Yao (1988). In the first step, the process of dropping a large number of equal-diameter cylinders in a container is simulated. Note that in the configuration so generated any cylinder is in contact with its nearest neighbors. Let ϕ_t be the solidity of such a closely packed random array. Berryman (1983) summarizes the results of several simulations and reports ϕ_t in the range of 0.81-0.89, with most studies quoting a value of approximately 0.82. Sangani and Yao (1988) have also simulated such arrays recently with upto 1600 cylinders in a container and they report a value of $\phi_t = 0.824$ and $Z = 4.2$. In the second step, the diameters of all the cylinder centers are shrunk by a constant amount $2\varepsilon r$, while keeping the location of all cylinder centers fixed. Here r is the bristle radius. The value of ε is chosen so that the new configuration has the measured solidity ϕ. For this special kind of array the gap between neighboring cylinders is uniform and is given by $2\varepsilon r$ where

$$\varepsilon = 1 - \left(\frac{\phi}{\phi_t}\right)^{1/2}$$

(7)

The resistance offered to the flow by the gap between pairs of nearly touching cylinders determine the overall drag and hence the effective permeability of the medium. The analysis below is due to Sangani (1990). The pressure drops as fluid squeezes through a gap of width $2\varepsilon r$ at a volume flow rate Q, as shown in figure 3. Here Q is the two-dimensional volume flow rate. The profile of the cylinder surface can be approximated by

$$\frac{f(x)}{r} \approx \varepsilon + \frac{x^2}{2r^2} \quad \text{for} \quad \frac{x}{r} \to 0 \ (\varepsilon^{1/2})$$

(8)

Assume that inertia terms are negligible and that the viscous forces in the streamise direction are small compared to those in the normal direction. Hence the equation governing the x- direction velocity component $\hat{u}$ reduces to

$$\mu \frac{\partial^2 \hat{u}}{\partial y^2} \approx \frac{dp}{dx}$$

(9)

Integrating the above equation with $\hat{u} = 0$ at $y = f(x)$ and $\partial\hat{u}/\partial y = 0$ at $y = 0$ we obtain

$$\hat{u} = -\frac{1}{2\mu} \frac{dp}{dx} [f^2(x) - y^2)]$$

(10)

Integrating the above velocity profile over the gap and identifying it with volume flow rate Q, we obtain

$$(\Delta p) \text{ gap} = \frac{9\pi\mu Q}{8\sqrt{2}} \frac{\varepsilon}{r^2}^{-5/2}$$

(11)

Thus the force exerted per unit length and width in direction of flow is Δp. The direction of flow however is normal to the line segment joining the centers of the cylinder pair in question. If such a line segment is oriented at an angle θ_i as shown in figure 4, then the force vector F_i per unit length arising over width 2r due to each gap for volume flow rate Q_i is given by

$$F_i = \frac{9\pi\mu Q_i}{8\sqrt{2}} \frac{\varepsilon_i^{-5/2}}{r^2} (2r)$$

(12)

The component of the force (per unit length) in the direction of mean flow (assumed to be along $\theta_i=0$) is then obtained after noting that $Q_i = (2\hat{u}\sin\theta_i) r$

$$F_{1i} = |F_i| \sin\theta_i = \frac{9\pi\mu\varepsilon^{-5/2}}{8\sqrt{2}} 2\hat{u}\sin^2\theta_i$$

(13)

Here $\hat{u}$ is the filter velocity or the superficial velocity. Hence, the mean force $<F_1>$ is given by

$$<F_1> = \frac{9\pi\mu\hat{u}Z}{8\sqrt{2}} \varepsilon^{-5/2}$$

(14)

where Z is the average number of nearest neighbors and the mean value of $\sin^2\theta_i$ averaged over all θ_i is 1/2. If the number of cylinders per unit cross-section area is $4\phi/\pi d_o^2$ where d_o is the diameter then

$$|\nabla p_1| = <F_1> \frac{4\phi}{\pi d_o} = \frac{9Z\phi\mu}{2\sqrt{2}} \varepsilon^{-5/2} \frac{\hat{u}}{d_o^2}$$

(15)

If one was interested in the permeability k of the medium defined as $k = \mu\hat{u}/|\nabla p|$ then

$$k = \frac{2\sqrt{2}}{9Z\phi} d_o^2 \varepsilon^{5/2}$$

(16)

which is identical to the expression in Sangani and Yao (1988) except for ϕ in the denominator.

2.3 Elastic Behavior Model

The expression in (15) permits us to calculate $|\nabla p|$, as a function of the filter velocity u which may vary along the bristle axis as given by (6). Hence, we are in a position to determine the loading on the bristle due to the inter-bristle flow driven by the Couette flow in the clearance region. We define a co-ordinate system shown in figure 5. The deflection of the bristle tip, Δ_t, can be obtained from straightforward application of linear elasticity theory. The radial component of the deflection $h_o = \Delta_t \cos\beta$ is then the clearance, and is given by

$$h_o = \Delta_t \cos\beta = \frac{9Z}{2\sqrt{2}} \varepsilon^{-5/2} \frac{\mu u_o}{\eta} \frac{\cos\beta}{(\sin\beta)^3} \frac{1}{EI} \frac{1}{\delta} \frac{h^3}{3}$$

(17)

Recall that $\eta = (1-\phi)(1+\lambda\delta h_o)$, $\delta = (\lambda k)^{-1/2}$, $I = \pi d_o^4/64$. Since the above equation is implicit in h_o, consider $h_o \gg k^{1/2}$ first, so that $\lambda\delta h_o \gg 1$ providing an explicit form,

$$\left(\frac{h_o}{d_o}\right)^2 = \frac{9Z}{2\sqrt{2}} \left[1 - \sqrt{\phi/\phi_t}\right]^{-5/2} \frac{\mu u_o}{(1-\phi)} \frac{k}{d_o^2} \frac{\cos\beta}{(\sin\beta)^3} \frac{h^3}{3EI}$$

(18)

If permeability k is experimentally determined for the medium then that measured value can be used in the above expression. The recommended values of ϕ_t

223

and Z are 0.82 and 4.2 for a random array of cylinders. Hence the expression is valid for $\phi < \phi_t(=.82)$. If, however, k is not known, permeability can be estimated from (16) allowing us to determine h_0 from

$$\left(\frac{h_o}{d_o}\right)^2 = \frac{\mu u_o}{\phi(1-\phi)} \frac{\cos\beta}{(\sin\beta)^3} \frac{h^3}{3EI} \qquad h_o >> \sqrt{k}$$

(19)

In the absence of any clearance h_0 vanishes and any initial increase in h_0 must occur with $h_0 << k^{1/2}$. Under circumstances that permit us to assume $\lambda \delta h_0 <<1$ we obtain

$$\frac{h_o}{d_o} = \frac{9Z}{2\sqrt{2}} \left[1 - \sqrt{\phi/\phi_t}\right]^{-5/2} \frac{\mu u_o}{(1-\phi)} \frac{\sqrt{\lambda k}}{d_o} \frac{\cos\beta}{(\sin\beta)^3} \frac{h^3}{3EI}$$

(20)

Once again k can either be measured or evaluated from equation (16). In the above expression in addition to Z and ϕ_t we also need an empirical estimate for the constant $\lambda^{1/2}$. The constant $\lambda^{1/2}$ can be identified with α in Beavers and Joseph (1967) and is a dimensionless quantity depending on the material parameters which characterize the structure of the porous medium within the boundary region where the filter velocity decays to zero, its Darcy value. The value of α reported by Beavers and Joseph are for Foametal and Aloxite, with effective pore sizes varying between 0.013 inches and .045 inches. The value of α for these materials was found to vary between 0.1 and 4 with lower values observed at lower pore sizes.

Preliminary estimates of the clearance due to tangential loading can be made from either (19) or (20) and if it turns out that h_0 is of the order of $k^{1/2}$ then the quadratic equation (17) can be solved for h_0. Before discussing the results for the tangential deflection we will develop the analysis for axial deflection. This will permit us to determine their relative magnitudes and establish conditions under which, it may be possible to neglect the clearance due to deflection in one of the directions.

3. Axial Deflection

The axial deflection of the bristles is due to the pressure differential along the axis of the rotating element. It is the purpose of the brush seal to minimize what would otherwise be a leakage flow due to this pressure differential. The axial loading on the bristle is straightforward to estimate since the pressure differential impressed upon the bristle bundle can be assumed to remain unaltered in the presence of leakage flow. If the pressure differential is $\Delta p = P_h - P_e$ over the width w of the

224

bristle bundle (in the axial direction) then the force per unit length, q, acting on the bristle is given by $q = \Delta p \, d_o^2/w$. This force acts uniformly over the overhanging length a of the bristle, i.e. exposed portion between the backing ring of inner diameter D_b and the shaft, diameter D_s. Since the bristle bundle is clamped at the retaining plate inner diameter D_r, the bristle behavior can be modeled as a bar clamped at origin and simply supported at D_b with an overhanging distributed load between D_b and D_s. If we define L to be the bristle length between the retaining ring ID and the backing ring ID, $L = (D_r - D_b)/2 \sin \beta$ then the bristle geometry with its axial loading diagram is as shown in figure 6. We wish to determine the displacement, Δ_h, due to the axial deflection of the unloaded member, as shown in figure 7. This quantity is the clearance produced due to the axial loading and would be observed in a static leakage test. In dynamic tests the clearance would be produced by a combination of effects, the tangential as well as the axial loading.

Linear elasticity theory assumes small angles of rotation for the beam and thus would only permit the calculation of the vertical displacement Δ_v while Δ_h would remain zero. Typical axial loading and the bristle length to diameter ratios are however, such that it becomes necessary to use large deflection theory in order to model the problem. Thus the differential equation of the deflection curve becomes

$$\frac{\left[\dfrac{d^2 y}{dx^2}\right]}{\left[1+\left(\dfrac{dy}{dx}\right)^2\right]^{3/2}} = -\frac{M(x)}{EI} \tag{21}$$

The exact shape of the elastic deflection curve given by the solution to this equation, is called the elastica. The mathematical solution to the problem of determining the elastica has been obtained for many different types of beams and loading conditions, see Frisch-Fay (1962). The solutions to the specific loading of interest here was not available in the existing literature. A particular difficulty is that the problem is statically indeterminate and the reaction force where the bristle is simply supported is unknown. While a linear theory may provide a value of the reaction, it will be approximate at best. This value, however, could be of use as an initial guess in an iterative determination of the reaction force into vertical component R and horizontal component $R\tan \theta$, where $\tan \theta$ is the bristle slope at the support, see figure 7. To determine Δ_h we need to solve for the elastica and

terminate the curve at a point where the length of the curve is (L + a). Here we assume that any elongation of the bristle is negligible or of an order smaller than that under consideration. In the deformed position of the bristle the axial loading is no longer applied over the overhang initial length 'a' but over the overhang length $a' = a - \Delta_h$ in the deformed position. The direction of the axial force, however, continues to remain vertical in the deformed position.

Solution to the problem described above requires us to integrate (21), with a moment distribution function M(x) given by

$$M(x) = qa' (a'/2 + L-x) -R(L-x) -R\tan\theta y \quad 0 < x < L$$

$$M(x) = (q/2) (L + a' - x)^2 \qquad L < x < L + a \qquad (22)$$

where a' and $\tan\theta$ are unknown and are determined as part of the solution y(x). The reaction force, however, is still unknown because the problem is statically indeterminate. This difficulty is easily overcome, especially since the solution is perhaps most easily obtained on a computer. An initial guess of R is made from linear theory. The preliminary solution thus obtained however, will in general fail to pass through the support at (L,0). The magnitude of the reaction force is gradually changed until the elastica does pass through, (L,0). It is convenient to normalize x and y with length L, i.e. $x^* = x/L$ and $y^* = y/L$. Dropping asterisk now equations (21) and (22) become

$$y''/(1+y'^2)^{3/2} = -M(x) \quad \text{with } y(o) = o \ y'(o) = 0, \text{ where}$$

$$M(x) = C_{eff} \left\{ 1/2 + (1/a') (1-x) \right\} - \alpha (1-x) - \alpha \tan\theta \, y \quad 0 < x < 1$$

$$M(x) = (C_{eff}/2) (1/a')^2 (1 + a'-x)^2 \quad 1 < x < 1 + a/L \qquad (23)$$

where $C_{eff} = C (a'/a)^2$, $C = qa^2L/EI$ and $\alpha = RL^2/EI$

The problem shown above was solved numerically for various values of the loading parameter C and the overhang ratio a/L. The elastica curves for a/L = 0.2 are shown in figure 8. Note that the axis in the y-direction is stretched considerably for clarity. The quantity of interest here is the clearance Δ_h the variation of which with loading parameter C is shown in figure 9 for several overhang ratios a/L. Note that the small deflection theory value of Δ_h is identically zero for all C. We observe that the departure from this value as loading is increased depends upon the overhang parameter. It turns out that for typical gas turbine applications brush seals may be operating in a parameter range where Δ_h is rapidly increasing with C and a/L.

The actual value of the reaction force is not of immediate interest once the axial deflection is known, however, it may be of use in the following manner. Earlier analysis to determine the circumferential deflection assumed that the friction at the bristle-backing ring interface was negligible. The bristle orientation under axial loading shown in figure 8 indicates that the only point of contact may be at the inner edge of the backing ring where the normal force acting on the bristle is given by $R/\cos \theta$. An estimated value of the static Coulomb friction coefficient would permit an approximate evaluation of the tangential restraining force. This force would act on the bristle layer in contact with the backing ring. While in this paper we do not account for this friction force in the calculation of the circumferential deflection the value of R and θ may prove useful for future work.

4. Discussion

Under dynamic conditions the actual deflection would be due to both the circumferential and axial loads and a vector sum of forces has to be used to solve the three-dimensional elastica problem. Additional simplification is possible if we can demonstrate that the deflection in one of the directions is small compared to the other. An explicit expression for their relative magnitude is not available because of the lack of a closed form formula for the axial deflection.

The numerical results of figure 9 establish that the behavior of Δ_h (C, a/L) is indeed nonlinear, and may be of importance in the design of brush seal systems. In addition to the expected non linearity in the response to loading parameters C the displacement h is also sensitive to a/L ratios. Thus it is not just the overhang length that is relevant even though it is the length exposed to a pressure differential but also the size of the retaining plate. The analysis carried out here while making several idealizations may provide insight into the dependence of the clearance on geometry and operating conditions.

BIBLIOGRAPHY

1. Beavers, G. S., and Joseph, D. D., "Boundary Conditions at a Naturally Permeable Wall", Journal of Fluid Mechanics, Vol. 30, 1967, pp 197-207.

2. Beavers, G. S., Sparrow, E. M., and Magnuson, R. A., "Experiments on Coupled Parallel Flows in a Channel and a Boundary Porous Medium", ASME Journal of Basic Engineering, Vol. 92, Series D, No. 1, 1970, pp. 843-848.

3. Berryman, J., Phys. Rev. A 27, 1983, p. 1053.

4. Flower, R., "Brush Seal Development System", AIAA paper 90-2143, 26th Joint Propulsion Conference, July 16-18, Orlando, Florida, 1990.

5. Frisch-Fay, R., "Flexible Bars", Butterworths, Washington, 1962.

6. Holle, G. F., and Krishnan, M. R., "Gas Turbine Engine Brush Seal Applications", AIAA paper 90-2141, 26th Joint Propulsion Conference, July 16-18, Orlando, Florida, 1990.

7. Rudraiah, N., "Coupled Parallel Flows in a Channel and a Bounding Porous Medium of Finite of Thickness", ASME Journal of Fluids Engineering, Vol. 107, 1985, pp. 322-328.

8. Sangani, A. S., Personal Communication, 1990.

9. Sangani, A. S. and Yao, C., "Transport Process in Random Arrays of Cylinders. Part II Viscous Flow", Physics of Fluids, Vol. 31, 1988, pp. 2435-2444.

10. Williams, W. O., "Constitutive Equations of a Flow of an Incompressible Viscous Fluid Through a Porous Medium", Quarterly of Applied Mathematics, 1978, pp. 255-267.
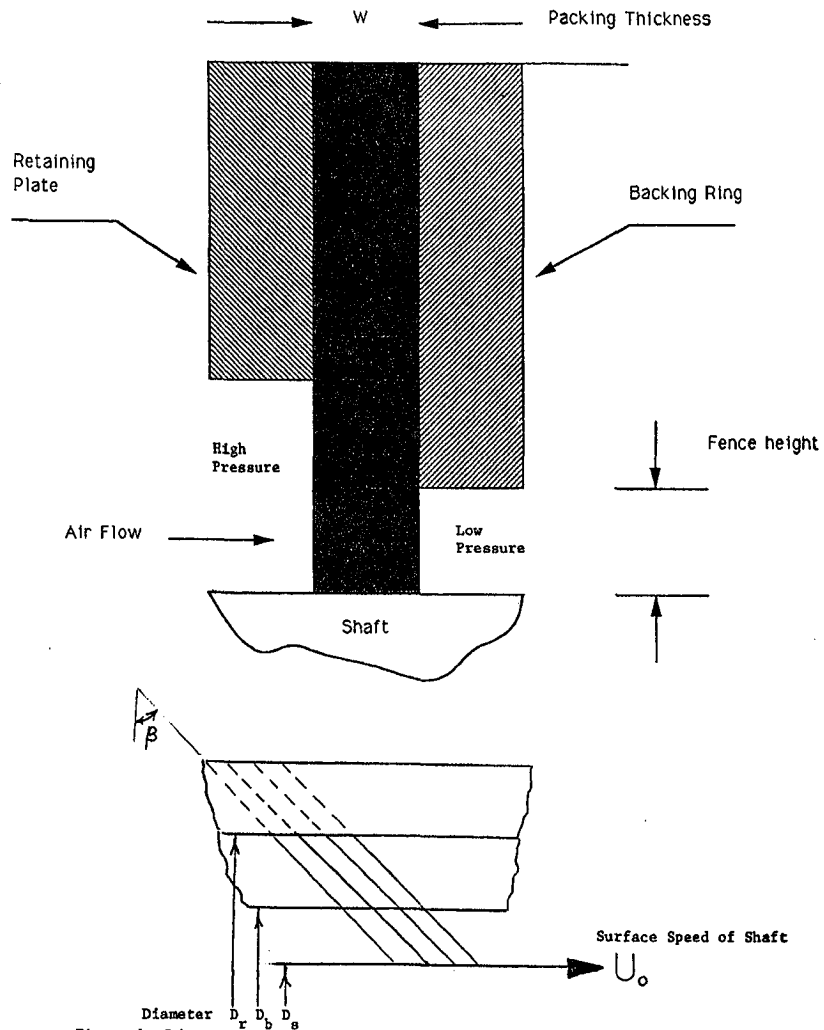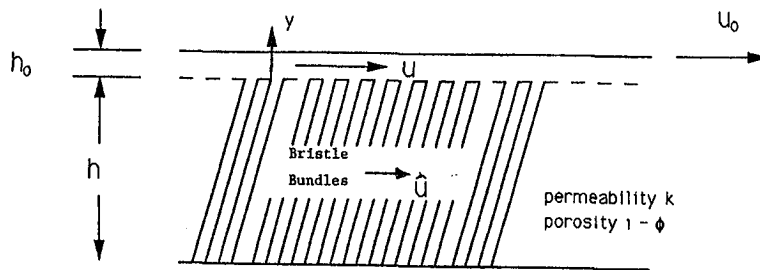
Figure 1   Schematic of Brush Seal System.

Figure 2

Physical model of clearance channel
bounded by shaft on one side and
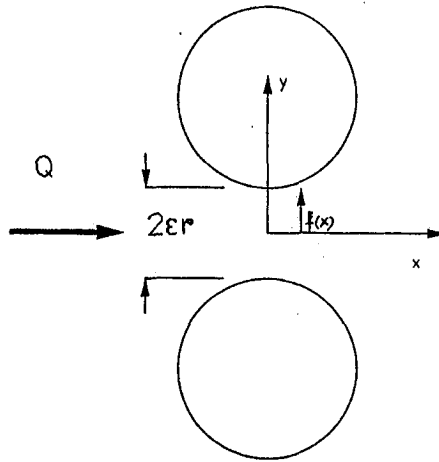porous bristle bundle on other.

Figure 3   Schematic of Volume Flow Q
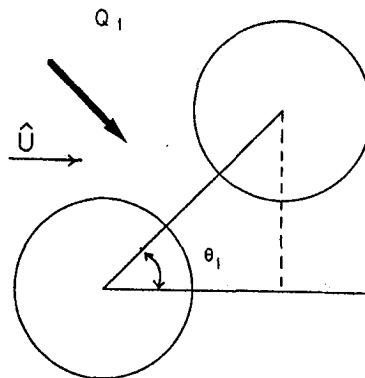through a gap of size $2\varepsilon r$

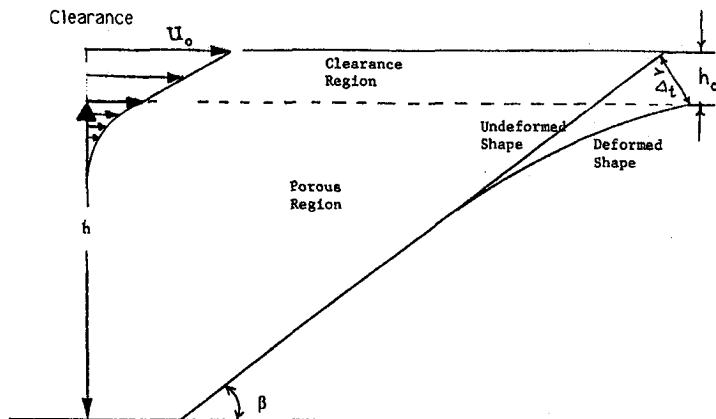Figure 4   A pair of neighbouring cylinders
in a random array.

Figure 5   Schematic diagram of clearance region and the porous
bristle bundle matrix. Velocity distributions in each
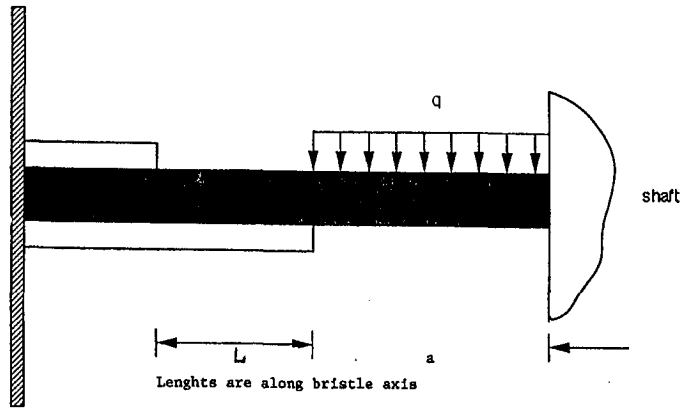are shown at left. Bristle displacement is normal to its
axis.

$$h_o = \Delta_t \cos \beta$$

Figure 6 Axial loading diagram for a single bristle.
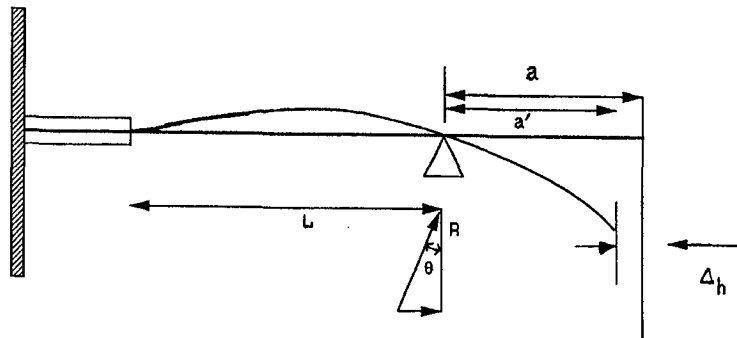
Figure 7 Schematic diagram showing the deformed shape of the bristle under axial loading. Horizontal displacement is such that the length of the bristle is unchanged under loading.
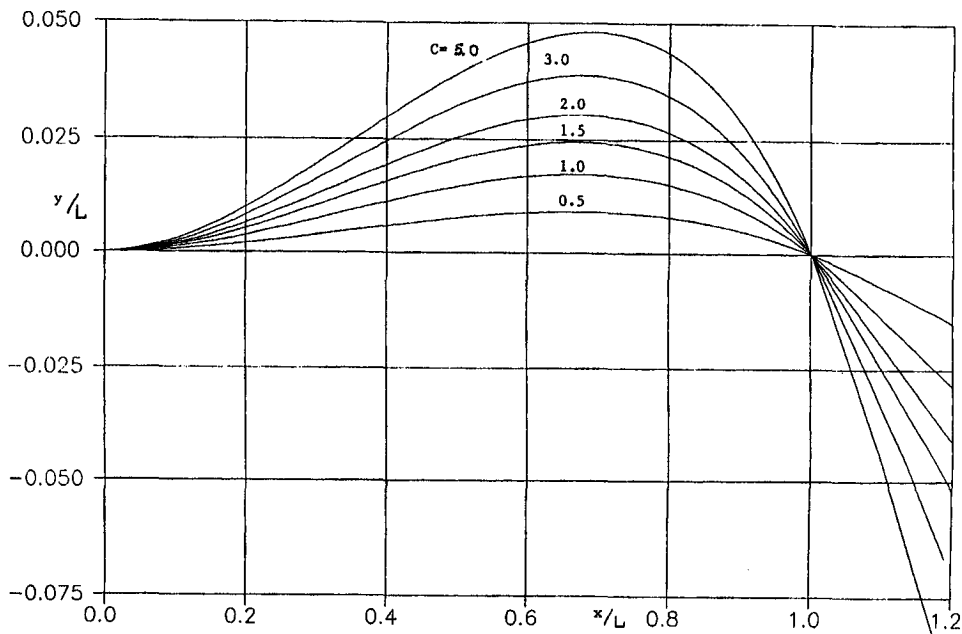

Figure 8 Computed Bristle shapes for axial loading C. The overharg ratio a/L =0.2.
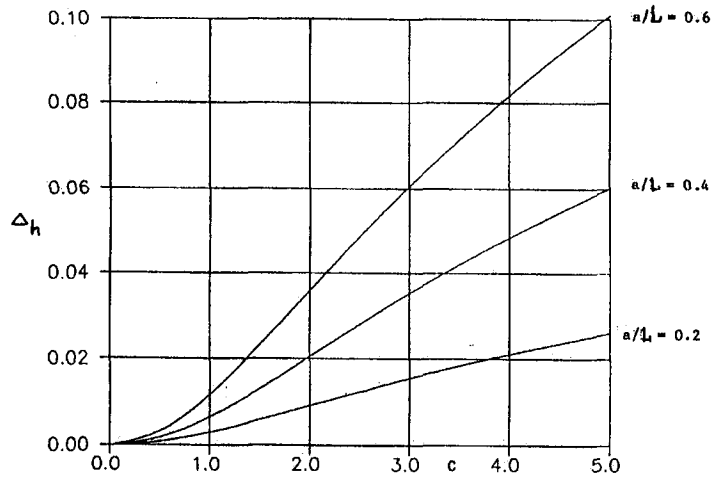
Figure 9 Clearance generated due to axial loading for various values of C. a/L = 0.2,0.4,0.6
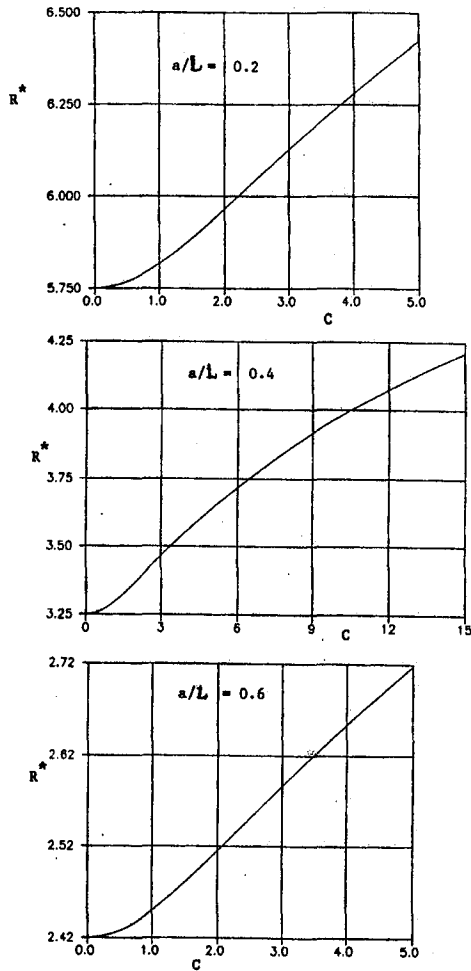

Figure 10 Variation of the Normalized reaction force R^* where $R^* = (RL^2/EI)/C_{eff}$